

# Measuring non-Kolmogorov turbulence

Szymon Gladysz, Karin Stein, Erik Sucher, Detlev Sprung

Fraunhofer Institute of Optronics, System Technologies and Image Exploitation, Gutleuthausstr. 1,  
76275 Ettlingen, Germany

## ABSTRACT

We have performed a series of experiments aiming at understanding the statistics of deep turbulence over cities. The experimental setup consisted of a Shack-Hartmann wavefront sensor and an imaging camera that simultaneously recorded wavefront-, and focal-plane data, respectively. At the same time, measurements of deep optical turbulence were performed at the urban area of interest using two large-aperture scintillometer systems to get an impression of the strength of  $C_n^2$  above the rooftops of Ettlingen. Our focus is “urban” turbulence because we are interested in the usefulness of adaptive optics for free-space optical communications over urban areas. We discuss methods of determining departure from Kolmogorov turbulence. Our “last mile problem” is that urban turbulence can be significantly stronger, in the sense of flatter power spectrum, compared to the classic Kolmogorov turbulence. This could pose a significant challenge for adaptive optics systems.

**Keywords:** Imaging through turbulence, adaptive optics, urban turbulence, free space optical communications

## 1. INTRODUCTION

Knowledge of statistics of atmospheric turbulence is essential for practical design of adaptive optics (AO) systems. The work of Kolmogorov<sup>1</sup>, Obukhov<sup>2</sup>, Tatarski<sup>3</sup>, Fried<sup>4</sup> and others has made it possible to model the performance of AO systems based on sound theory. All AO systems are being designed based on the Kolmogorov model. Focus of the Adaptive Optics Group at Fraunhofer IOSB is on atmospheric compensation for free-space laser communications. In communications, the figure of merit is the bit-error rate (BER) and predictions of AO performance in terms of this metric have been calculated, again based on the Kolmogorov model<sup>5</sup>. How effective could AO be in non-Kolmogorov turbulence remains an answered question, both theoretically and experimentally.

Secondly, it is well known that various mirror-, or Zernike-modes, employed in modal control, could be compensated with various bandwidths and/or gains<sup>6</sup>. This is the principle of modal gain optimization. Such analyses have again been performed based on the Kolmogorov model. For the holographic wavefront sensor we are building<sup>7</sup>, which by default employs modal compensation in parallel channels, implementation of modal gain optimization would be straightforward. Still, as free-space laser communications systems would be deployed in urban areas and close to roof-tops, chimneys, heat sources, etc. – where the applicability of Kolmogorov’s assumptions might be limited – it is worthwhile to check the slope of the measured spectrum and use this empirical spectrum in theoretical investigations of the optimal AO bandwidth. To summarize, our interest in non-Kolmogorov turbulence stems from the intention to model: 1) bit-error rate after AO, and 2) optimal AO bandwidth for each Zernike mode for a system deployed in an urban environment.

First important work on non-Kolmogorov turbulence in the optics literature, which introduced notation and theoretical framework subsequently used by other authors, is the paper by Stribling et al.<sup>8</sup> First experimental method for measuring non-Kolmogorov turbulence has been proposed by Nicholls et al.<sup>9</sup> Effects of generalized atmospheric turbulence on the performance of laser-communications or imaging systems have been quantified by Kopeika et al.<sup>10</sup>. Theoretical work resulting in expressions for beam wander, probability of fade and BER was recently published by Toselli<sup>11,12</sup>.

Very few experimental results have been published on non-Kolmogorov turbulence. Of particular value are the measurements of the exponent of the refractive index power spectrum (or alternatively, of the exponent of the phase structure function). These scarce measurements have mostly shown spectra flatter than the Kolmogorov model when the occurrence of non-Kolmogorov turbulence had been observed<sup>13</sup>. Steeper spectra have not been reported. This is also the

case with our results. Additionally, an indirect but significant observation of departures from the Kolmogorov model over a 149 km path has been reported by Vorontsov et al. <sup>14</sup> In these experiments it has been shown that the assumption of "frozen" turbulence (Taylor hypothesis), commonly used to switch between theories in spatial and temporal domains, can rarely be justified over very long propagation paths. Additionally, for three tested wavelengths, dependence of the intensity scintillation variance on wavelength did not follow existing assumptions that the longer the wavelength the less the turbulence effect on the laser beam.

In micrometeorology, wind velocity and temperature spectra in urban environments have been compared to the theoretical slopes in the inertial subrange stemming from the Kolmogorov model. For example, the analysis of power spectra, obtained in the urban surface layer above the city of Basel <sup>15</sup>, indicate that the assumption of isotropy would fail when analyzing the ratio of wind spectra in two orthogonal directions extracted from sonic anemometer measurements. On the other hand, the slopes of the temperature spectra revealed expected behavior. The height of the measurements was 1.32 times the average rooftop height of this urban area <sup>15</sup>. In an overview article on the subject the dependence of the slope of the temperature spectra on height above ground was shown and discussed <sup>16</sup>. Close to the rooftop level the slope postulated by Kolmogorov was not found. Kolmogorov model seems to be fulfilled from about 1.3 - 1.6 times of the rooftop level in the urban surface layer.

Apart from the point measurements with ultrasonic anemometers, scintillometers have been traditionally used to measure deep optical turbulence over cities. Here the main focus has been on the derived sensible heat fluxes. The analyses of  $C_n^2$  have not been pursued <sup>17</sup>. Some measurements of the integrated optical turbulence over cities with a surface layer scintillometer have been published <sup>15</sup>. To partially fill this gap we have performed measurements of the turbulence character using two large-aperture scintillometer systems. The results should provide some information above the strength of optical turbulence and the representativeness of our measurements in respect to basic research on the type of urban turbulence.

## 2. METHODS

The exponent of the refractive index power spectrum, which for the two- and three-dimensional spectra is  $-11/3$  in the Kolmogorov model, can be measured directly or indirectly. The indirect methods rely on the validity of the Taylor hypothesis mentioned above. Since high-spatial-resolution measurement of refractive index or phase is challenging, temporal-domain measurement of a related quantity like angle-of-arrival or single-point phase is usually performed. There exist theories linking the refractive index or phase power spectra to derivative quantities <sup>6</sup>.

Naturally, it is always better to perform a direct measurement. To our knowledge only one such method exists. It is based on the relationship between the angle-of-arrival covariance (measurable) and the non-Kolmogorov phase structure function. Measurement of the former quantity can be performed with a Shack-Hartmann wavefront sensor (SHS) <sup>9</sup>. The method is straightforward and elegant. Its range of applicability is wide because even for scenarios involving strong turbulence near the ground, whereby SHS is susceptible to scintillation and wavefront reconstruction failure rate is high <sup>18,19</sup>, it is still possible to find the positions of remaining spots and so the calculation of the angle-of-arrival covariance is possible, even if wavefront reconstruction process fails.

In this paper we present indirect measurements of departures from Kolmogorov/Taylor-flow predictions. Specifically, we focus on 1) temporal spectra of image motion (angle-of-arrival fluctuations) which for spherical-wave propagation should have the  $-11/3$  exponent according to the Kolmogorov model <sup>6</sup>, 2) temporal spectra of the amplitudes of Zernike polynomials reconstructed from the SHS spots positions, which again should follow the  $-11/3$  law <sup>6</sup>. Rather than making general statements about the statistical properties of turbulence over our experimental paths we focus in this paper on the methodology of measuring possible departures from the Kolmogorov model. We list various technical obstacles and sources of possible misinterpretations and hope that our methodologies can serve the optical-turbulence community in future experiments.

### 2.1 Image motion and wavefront measurements

Experiments were carried out at Fraunhofer IOSB in Ettlingen, Germany, over 2.6 and 2.9 km experimental paths on several days during daytime in 2012 and 2013 during the months of January, March, August, and November. The experimental paths cover urban area of downtown Ettlingen, a few fields and a small portion of the forest (Figure 1). In majority of experiments beacons were implemented as follows: Holes of diameters ranging from 1 to 5 cm were cut in opaque masks and these masks were placed, sequentially, in front of a 2000 W (max power) lamp of aperture equal to

about 20 cm. The lamp was operated by a technician and set up on a small hill facing the Institute. The 5-cm source is already anisoplanatic for the  $C_n^2$  values measured during the experiments. In the last experiment, on August 29<sup>th</sup> 2013, we worked with a true point source: a red (625 nm) LED from Osram with luminous flux output of 165 lm. Combined with a lens (Carclo,  $\varnothing = 20$  mm) this LED has a nominal angle of dispersion of 7.2°. On that day haziness hampered the operation of the SHS and only speckle images were collected with a camera.

The receivers are located inside the Adaptive Optics Laboratory, about 1 m from the (open) windows, at a height of approximately 20 m above ground. The lamp/LED was located at a height of approximately 50 m. Light from the source was collected with an 18 cm telescope and directed, through five relay lenses and mirrors, to a beam-splitter which divides the light between the wavefront sensor (Shack-Hartmann type; model Optocraft SHSfast based on the Photon focus MV1-D1312 CMOS Camera; 13×13 lenslets; 256×384 pixels in the focal plane) and the 8-bit imaging camera. When operated simultaneously, the wavefront sensor receives 97% of the incoming light, while the camera receives 3% of the light. In the experiment on August 29<sup>th</sup> 2013 all of the light was re-directed to the camera because SHS had problems locating spots in low signal-to-noise conditions on that day.

In order to work with monochromatic light, a narrow-band filter (650-700 nm) was placed in front of the imaging camera when working with white-light sources. When using the LED no filter was used. The camera was running at either 125 or 250 fps. Exposure times were set to either 2 or 4 ms. Turbulence strength,  $C_n^2$  estimated from image motion<sup>20</sup>, was around  $10^{-14}$  m<sup>-2/3</sup> during the experiments. Interestingly, scintillometer (BLS900 from Scintec, Rottenburg/Germany) taking measurements over the same path and during the same time reported values which were between 5 and 10 times lower. This is due to the difference in weighting functions of the two devices/methods. The scintillometer measures turbulence in the middle of the path while the camera is more sensitive to phase errors and therefore measures turbulence close to the sensor (away from the source). Turbulence inside the laboratory was qualitatively evaluated by taking fast-speed images of laser source positioned at the focus of the telescope. In most cases image motion due to laboratory conditions was an order of magnitude smaller than the turbulence-induced motion.

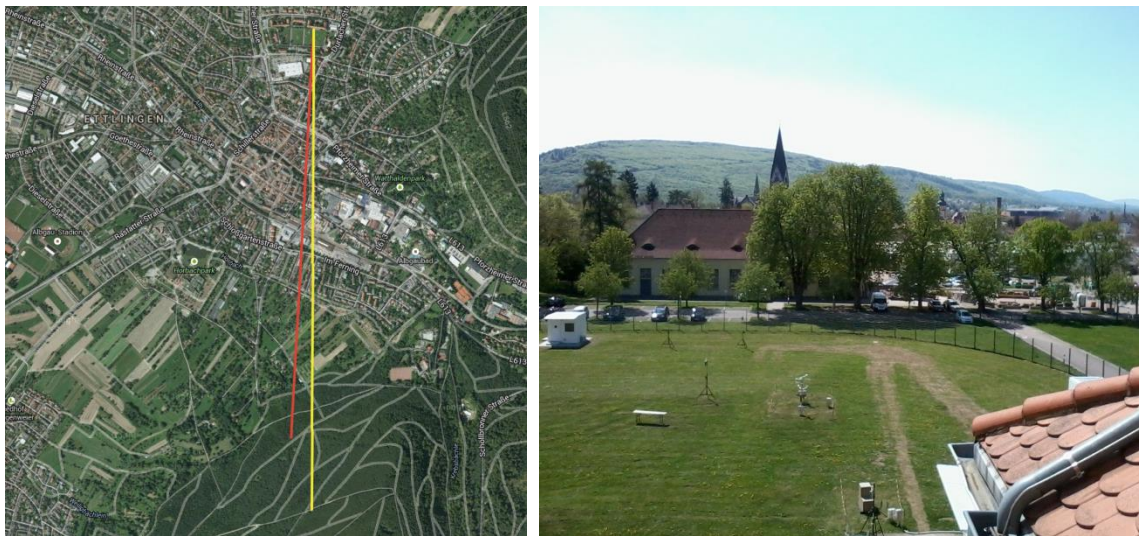


Figure 1. Left: aerial view of the experimental paths between Fraunhofer IOSB (top of the picture) and the locations of the beacons (at the bottom of the picture). Red denotes the 2.6 km path and yellow is the 2.9 km path. Map courtesy of Google. Right: view from the laboratory window.

Shack-Hartmann wavefront sensor was running simultaneously with the imaging camera. The SHS outputs coefficients of the first 15 Zernike modes, up to spherical aberration. Typically 2000 samples were collected at a speed of either 360 or 1000 Hz for the results presented in this paper.

## 2.2 Scintillometer measurements

Urban turbulence in the surface layer above the roof-tops was measured along three paths above Ettlingen with two large-aperture or boundary-layer scintillometers (BLS900). The BLS900 measures the integrated turbulence between a

transmitter and its receiver for distances between 500 m and 6 km. The transmitter consists of 2 disks with 924 LEDs each, out of which 36 visible-light LEDs are used for alignment and 888 LEDs operating at the wavelength of 880 nm are used for measurement. The intensity fluctuations of the beams from the two disks are measured at the receiver. From the covariance of the scintillations  $C_n^2$  is determined. Temporal resolution was set to 1 minute. Pulse repetition rate of 25 Hz was chosen. As already mentioned, BLS900 and similar scintillometers assign more weight to turbulence at the center of the measurement path.

Locations of the transmitter and receiver and the three measurement paths above Ettlingen are shown in Figure 2. Scintillometer measurements were performed continuously on periods of several days between April and August 2013 along the path from the tower of the fire station to Fraunhofer IOSB (purple in Figure 2). The distance was 2.6 km and the mean height at the center of the path was about 30 m above ground. There, the roof-tops layer was about 12 m. For comparison additional measurements were carried out in July on the path from the IOSB to Kreuzelberg (red in Figure 2). The path length was 2.6 km and the mean altitude above ground was around 42 m. The slope of the path was much steeper than before. Additional measurements were carried out in August between the tower of the station and the Bismarck Tower (Bismarckturm). The distance was 3.2 km and the height above ground 73 m.



Figure 2. Left: boundary layer scintillometer BLS900 (top left: transmitter, bottom left: receiver). Right: aerial view of the paths of the three scintillometer measurements: purple line from the Fraunhofer IOSB (A, receiver) to the tower of the fire station (B, transmitter), red line from the Fraunhofer IOSB (A, receiver) to the Kreuzelberg (C, transmitter), and cyan from tower of the fire station (B, receiver) to the Bismarck Tower (D, transmitter). Map courtesy of Google Earth.

### 3. DATA PROCESSING AND RESULTS

Typically the camera records sequences of length 510 frames. Subarray 3-D data-cubes of size  $300 \times 300 \times 510$  were extracted from the larger images, and background was subtracted. Bad pixels were removed. Very high-frequency stripe noise was removed with a simple Fourier filter. For each run, 3-D data-cubes and long exposures were saved in raw FITS (Flexible Image Transport System) format. Subsequently, image motion was estimated by up-sampled (4 times) cross-correlation with a reference image (long exposure shifted manually to the origin). Values of image motion, in pixels and in radians, were saved in text files. Angular pixel scale was estimated by recording images of two small lamps separated by a known distance. Finally, autocorrelations and power spectra of image motion were computed from the text files containing values of image displacements. Figure 3 shows a typical autocorrelation curve and Figure 4 presents power spectra based on a set of four arbitrarily chosen sequences. Both figures correspond to the experiment on August 29<sup>th</sup> 2013 when the LED was used as a beacon.

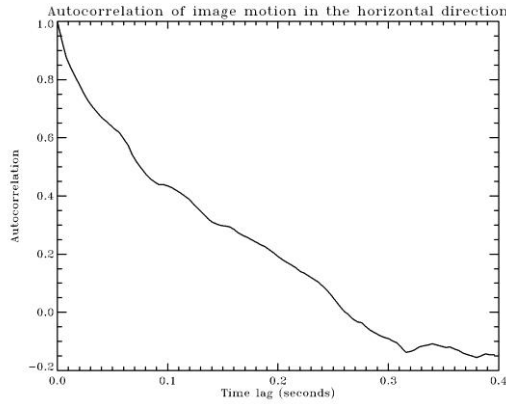


Figure 3. Typical shape of autocorrelation of image motion.

Figure 4 suggests non-Kolmogorov behavior. Because turbulence was very stable on the day of the observations we decided to average power spectra corresponding to the same camera settings (sensitivity and frame rate). In Figure 5 we show these average power spectra, both obtained from five homogeneous sequences, for the 125 fps and 250 fps cases. Here both the input and average power spectra were additionally smoothed with a window of width equal to ten frequencies. It is clear turbulence was not conforming to the Kolmogorov-Taylor-flow model.

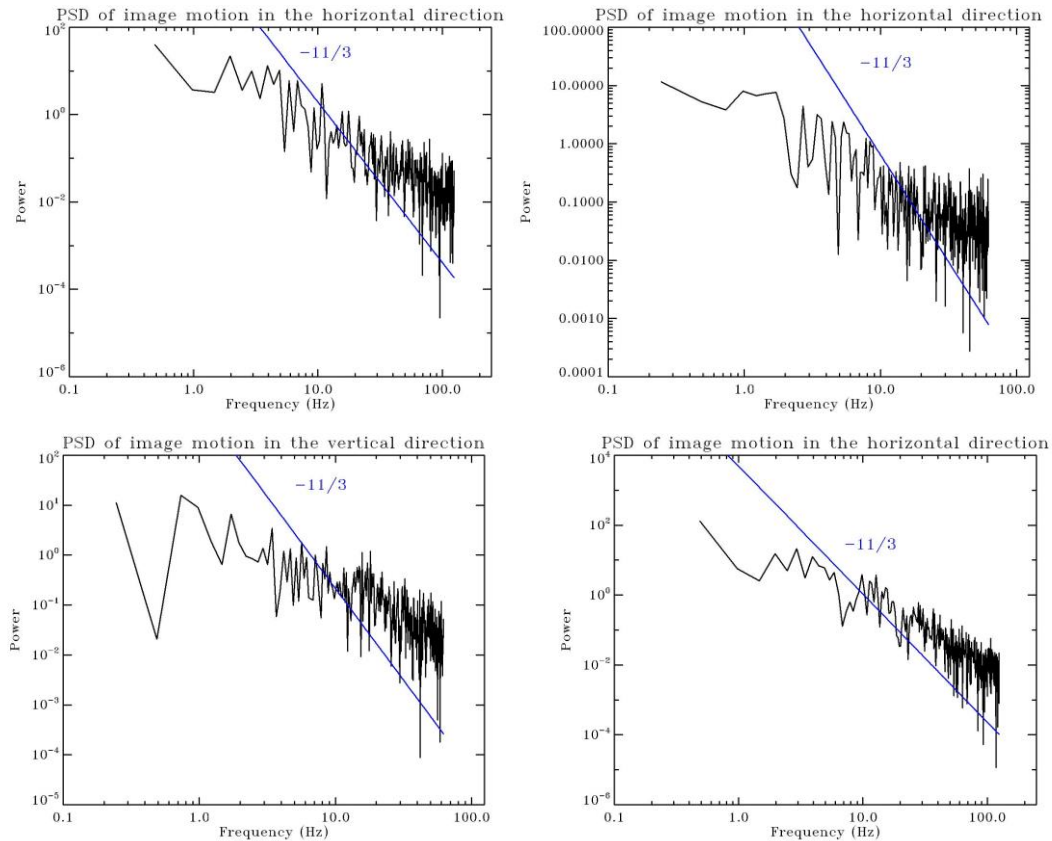


Figure 4. Temporal power spectra of image motion for four chosen datasets. The  $-11/3$  lines correspond to Kolmogorov turbulence and Taylor frozen flow <sup>6</sup>.

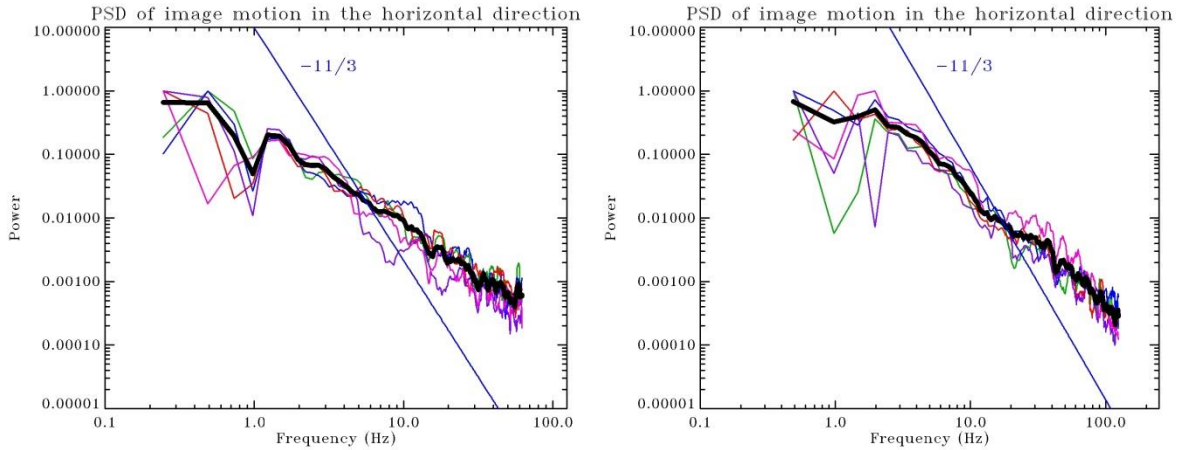


Figure 5. Temporal power spectra of image motion. Left: from five datasets taken at 125 fps. Right: from five datasets taken at 250 fps. Colors: individual smoothed power spectra. Thick black lines: averaged smoothed power spectra.

Departures from the Kolmogorov model were less obvious in the SHS measurements. Only a few experiments in weaker turbulence allowed for continuous reconstruction of all 15 Zernike modes. On other occasions SHS returned results which, upon visual inspection of their temporal behavior, were discarded as they were clearly noise (scintillation) dominated.

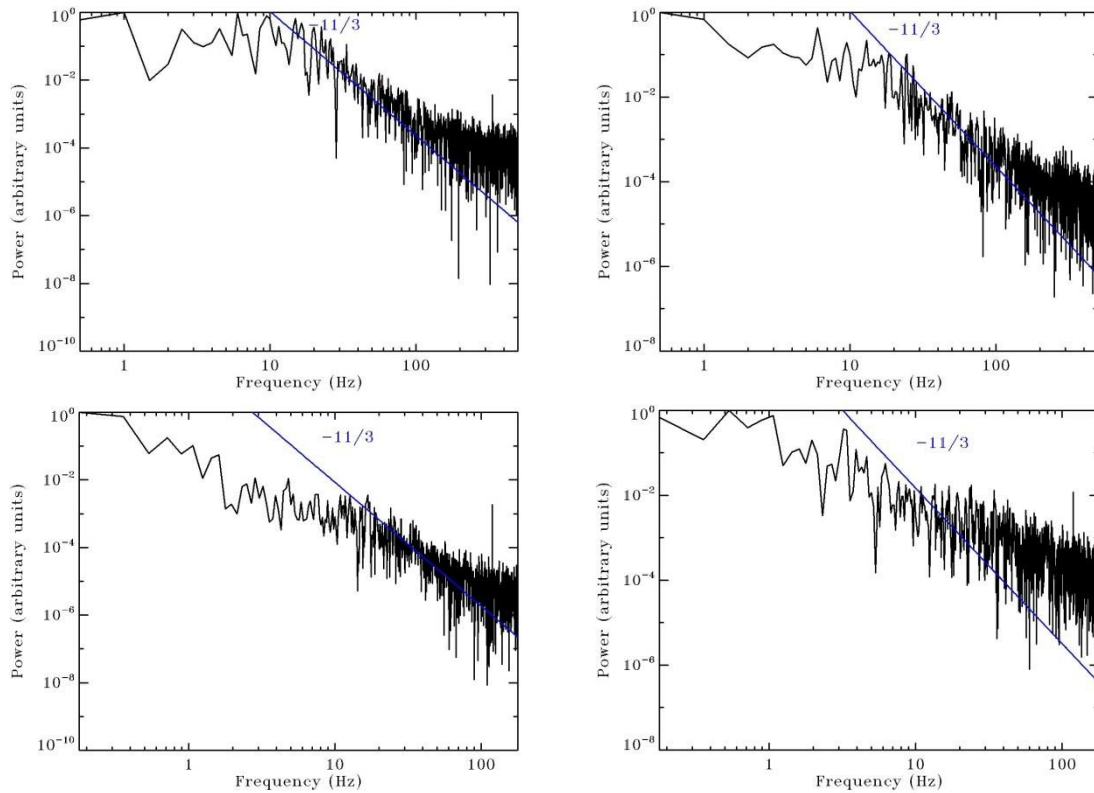


Figure 6. Temporal power spectra of Zernike polynomials. Top: experiments on March 21<sup>st</sup> 2013 (SHS frame rate = 1000 Hz). Bottom: experiments on February 21<sup>st</sup> 2013 (SHS frame rate = 360 Hz). Top left - defocus and top right - coma, bottom left - defocus and bottom right - spherical aberration. The  $-11/3$  lines correspond to Kolmogorov turbulence and Taylor frozen flow<sup>6</sup>.

In Figure 6 we show examples of power spectra which clearly conform to the Kolmogorov-Taylor-flow model (top) and also those which show flatter decays (bottom). Analysis of the dependency of the spectral slope on meteorological conditions has been undertaken but no distinct link has been found showing the validity of the  $-11/3$  slope postulated by the Kolmogorov model.

Additional goal of this research is to characterize our experimental site, the layer above the rooftops of Ettlingen. Measurements of deep optical turbulence were performed along the measurement path linking Fraunhofer IOSB and Kreuzberg (Figure 1 and Figure 2 (A-C)). Additional measurements were performed along two measurement paths across Ettlingen shown in Figure 2. This was done in order to ascertain the representativeness of our chosen path for urban turbulence character. Figure 7 shows the  $C_n^2$  time series for the IOSB-fire-station path for four weeks in 2013 between April and August. In close to clear sky conditions (for example 24<sup>th</sup>-25<sup>th</sup> April, 5<sup>th</sup>-6<sup>th</sup> May, or 1<sup>st</sup>-2<sup>nd</sup> August) the highest daytime values of  $C_n^2$  of about  $5$  to  $7 \times 10^{-14} \text{ m}^{-2/3}$  are observed, showing similar behavior throughout spring and summer. Nighttime values are often of the same order as the daytime values indicating the “heat island” effect<sup>16</sup>, which is responsible for unstable conditions at night and thereby also turbulence production. A maximum value of  $7 \times 10^{-13} \text{ m}^{-2/3}$  was measured for such a “heat island” night, from the 25<sup>th</sup> to 26<sup>th</sup> April 2013. The average height of the center of the path was 30 m, corresponding to about 2.5 times the rooftop level of this area.

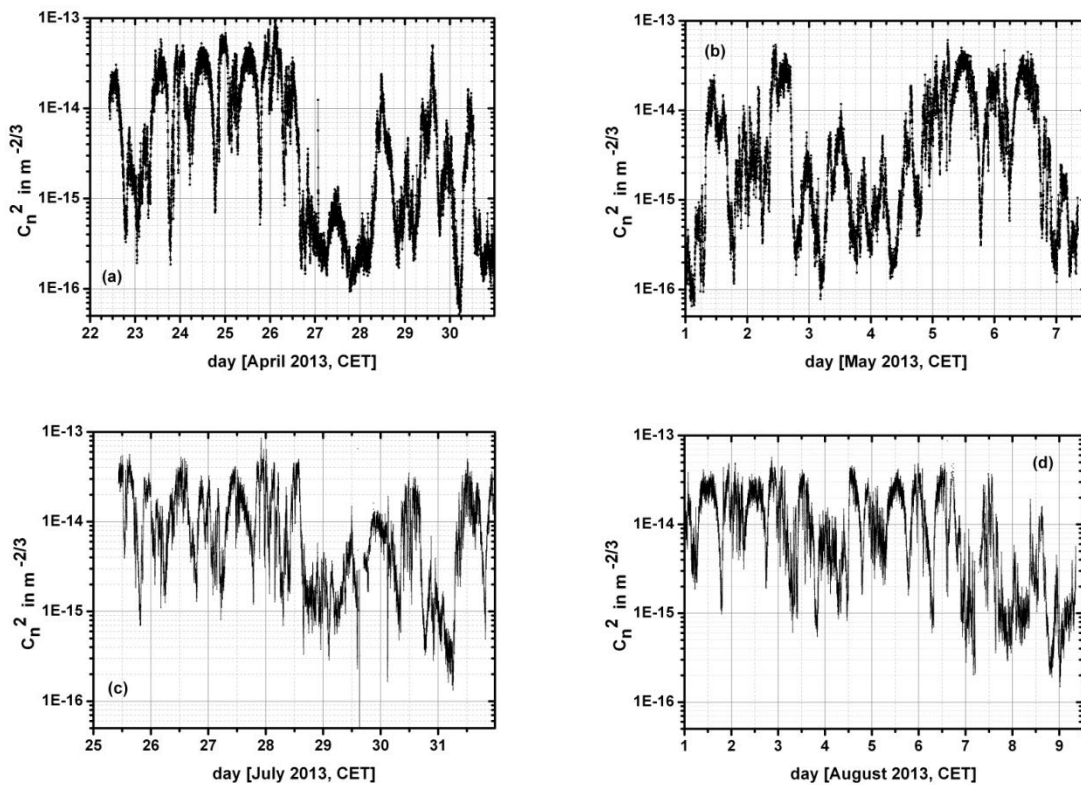


Figure 7. Time series of  $C_n^2$  for the 22<sup>nd</sup> to 30<sup>th</sup> of April 2013 (a), 1<sup>st</sup> to 7<sup>th</sup> of May 2013 (b), 25<sup>th</sup> to 31<sup>st</sup> of July 2013 (c) and 1<sup>st</sup> to 9<sup>th</sup> of August 2013 (d) for the measurement path from the fire station (transmitter) to the Fraunhofer IOSB (receiver), distance 2.6 km (purple in Figure 2), mean height 30 m above ground.

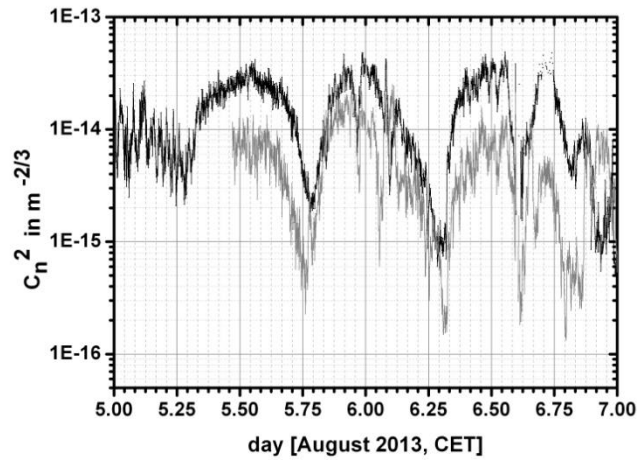


Figure 8. Time series of measurements from the 5<sup>th</sup> to the 8<sup>th</sup> of August 2013 Institute-fire station (black) and Bismarckturnm-fire station (grey).

In Figure 8 we compare turbulence measurements between two paths: Fraunhofer IOSB-fire station (black) and Bismarckturnm-fire station (cf. Figure 2). Values of  $C_n^2$  are in general lower for the Bismarckturnm-fire-station path. This could be expected because the mean height at the center of this path was about 73 m: twice as high as the other path. One can also note that measurements along the two paths exhibit similar daily behavior. Quite different were the results of comparison in the case of measurements shown in Figure 9. This time, the Institute-fire-station path exhibited lower turbulence than the Institute-Kreuzelberg path. The measurements show more noise, too. These two special behaviors are attributed to the disturbance by local effects (the line of sight seemed to be disturbed quite often). The path from Fraunhofer IOSB to Kreuzelberg was steeper and more slanted than the other two paths. The height difference between receiver and transmitter was more than 100 m. Therefore the question arises where along the path lies the point of interest for turbulence measurement? What effects are responsible for the contribution to the integrated value of  $C_n^2$ ? Future experiments will shed more light on these issues.

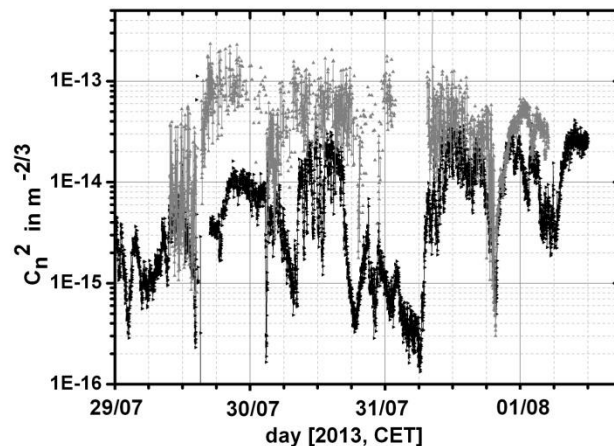


Figure 9. Time series of measurements from the 29<sup>th</sup> of July to the 1<sup>st</sup> of August 2013 IOSB-fire station (black) and IOSB-Kreuzelberg (grey).

## 4. FUTURE EXPERIMENTS

Before describing our future plans regarding turbulence characterization we will list various pitfalls which in our experience have to be considered when trying to measure non-Kolmogorov turbulence, especially in inhomogeneous urban environment. Sources of possible errors include:

- **anisoplanatic sources;** Care has to be taken to design experiments around sources not extending the isoplanatic angle, ideally lasers or LEDs. Naturally, then rises the problem of low signal-to-noise ratio when only low-power lasers can be deployed (often the case in urban environments).
- **laboratory turbulence;** When measuring turbulence with a wavefront sensor, one has to keep in mind that such a sensor will be sensitive to phase aberrations at the end of the path. Laboratory “seeing” can be non-Kolmogorov but care has to be taken to avoid interpreting the results as describing the whole propagation path.
- **too low frequency of the sensors;** Both – cameras and wavefront sensors have to be operated at speeds of the order of hundreds of Hz. Integration times have to be on the order of ms.
- **scintillation;** Results of wavefront reconstruction should be inspected visually for possible influence of scintillation on the measurements which makes them invalid.
- **frozen-flow hypothesis;** When making temporal measurements one has to remember that translating them into spatial domain is always based on the validity of the frozen-flow hypothesis.

We believe that in our future experiments we will be able to avoid all these pitfalls. Schematic showing the setup to be ready in late 2013 is in Figure 10. Laser light will be transmitted through a 30 cm telescope in the direction of the church steeple located 411 m in front of the Institute building. The retroreflector mounted at a column of the steeple will return the light back to the laboratory. The beam-splitter behind the telescope will re-direct a portion of light to the SHS and a portion to the camera recording pupil-plane images (scintillation). From the focal plane of SHS we will measure directly the angle-of-arrival covariance and find the exponent of (possibly non-Kolmogorov) power spectrum, without resorting to wavefront reconstruction<sup>9</sup>. The measured spectrum can then be plugged into theoretical expressions for scintillation index of Gaussian beam waves in weak turbulence<sup>21</sup> and checked against measurements from the camera. The short path of our experiment, corresponding to Rytov variance around 0.4, is therefore an advantage allowing us to use weak-fluctuation theory when necessary to explain departures from the Kolmogorov model. Strong-fluctuation theory is not fully developed yet.

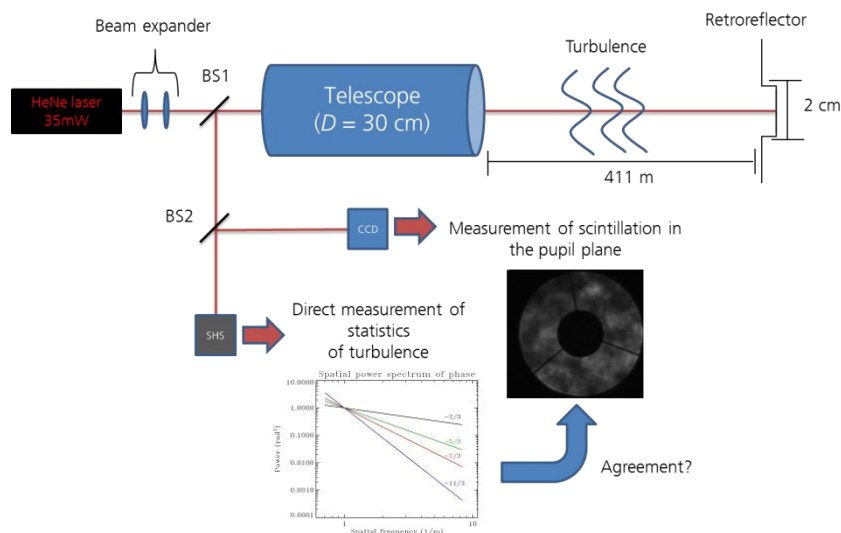


Figure 10. Schematic of the future experiment.

## REFERENCES

- [1] Andrey Kolmogorov, "The local structure of turbulence in incompressible viscous fluids at very large Reynolds numbers," *Dokl. Akad. Nauk. SSSR* 30, 299-303 (1941).
- [2] Alexander Obukhov, "Structure of the temperature field in turbulent flows," *Izv. Geogr. Geophys.* 13, 58-69 (1949).
- [3] Valerian I. Tatarski, *Wave Propagation in a Turbulent Medium* (McGraw-Hill Book Company, Inc., New York, 1961).
- [4] David L. Fried, "Optical resolution through a randomly inhomogeneous medium for very long and very short exposures," *J. Opt. Soc. Am.* 56, 1372-1379 (1966).
- [5] Robert K. Tyson, "Bit-error rate for free-space adaptive optics laser communications," *J. Opt. Soc. Am. A* 19, 753-758 (2002).
- [6] Jean-Marc Conan, Gérard Rousset, and Pierre-Yves Madec, "Wave-front temporal spectra in high-resolution imaging through turbulence," *J. Opt. Soc. Am. A* 12, 1559-1570 (1995).
- [7] Andreas Zepp, "Holographic wavefront sensing with spatial light modulator in context of horizontal light propagation," *Proc. SPIE* 8535, 85350I (2012).
- [8] Bruce E. Stribling, Byron M. Welsh and Michael C. Roggemann, "Optical propagation in non-Kolmogorov atmospheric turbulence," *Proc. SPIE* 2471, 181-196 (1995).
- [9] T.W. Nicholls, G. D. Boreman, and J. C. Dainty, "Use of a Shack–Hartmann wave-front sensor to measure deviations from a Kolmogorov phase spectrum," *Opt. Lett.* 20, 2460-2462 (1995).
- [10] Norman S. Kopeika, Arkadi Zilberman and Ephim Golbraikh "Generalized atmospheric turbulence: implications regarding imaging and communications", *Proc. SPIE* 7588, 758808 (2010).
- [11] Italo Toselli, Larry C. Andrews, Ronald L. Phillips, and Valter Ferrero, "Angle of arrival fluctuations for free space laser beam propagation through non-Kolmogorov turbulence," *Proc. SPIE* 6551, 65510E (2007).
- [12] Italo Toselli, Larry C. Andrews, Ronald L. Phillips, and Valter Ferrero, "Freespace optical system performance for laser beam propagation through non-Kolmogorov turbulence," *Opt. Eng.* 47, 026003(2008).
- [13] Ephim Golbraikh, Herman Branover, Norman S. Kopeika, and Arkadi Zilberman, "Non-Kolmogorov atmospheric turbulence and optical signal propagation," *Nonlin. Processes Geophys.* 13, 297 (2006).
- [14] Mikhail Vorontsov et al., "Characterization of atmospheric turbulence effects over 149 km propagation path using multi-wavelength laser beacons," *Proceedings of the Advanced Maui Optical and Space Surveillance Technologies Conference*, E18 (2010).
- [15] Matthias Roth, J.A.Salmond, and A.N.V. Satyanarayana, "Methodological considerations regarding the measurement of turbulent fluxes in the urban roughness sublayer: the role of scintillometry," *Boundary-Layer Meteorol.*, 121, 351-375 (2006).
- [16] Matthias Roth, "Review of atmospheric turbulence over cities," *Q. J. R. Meteorol. Soc.*, 126, 941-990 (2000).
- [17] Jean-Pierre Lagouarde, M. Irvine, J.-M. Bonnefond, C.S.B. Grimmond, N. Long, T.R. Oke, J.A. Salmond, and B. Oferle, "Monitoring the sensible heat flux over urban areas using large aperture scintillometry: Case study of Marseille City during ESCOMPTE experiment," *Boundary-Layer Meteorology*, doi 10.1007/s10546-005-9001-0 (2005).
- [18] Charles A. Primmerman, T. R. Price, R. A. Humphreys, B. G. Zollars, H. T. Barclay, and J. Herrmann, "Atmospheric-compensation experiments in strong-scintillation conditions," *Appl. Opt.* 34, 2081 (1995).
- [19] Gabriele Marchi and Corinne Scheifling, "Turbulence compensation for laser communication, imaging on horizontal path and non-natural turbulence using direct and iterative procedures," *Proc. SPIE* 8520, 85200C (2012).
- [20] Szymon Gladysz and Roberto Baena Gallé, "Comparison of image restoration algorithms in the context of horizontal-path imaging," *Proc. SPIE* 8355, 83550X (2012).
- [21] Italo Toselli, Larry C. Andrews, Ronald L. Phillips, and Valter Ferrero, "Free space optical system performance for a Gaussian beam propagating through non-Kolmogorov weak turbulence," *IEEE Transactions on Antennas and Propagation* 57, 1783 (2009).